

Antioxidant activity, DFT-calculation, and docking of 5-amino-*N*-(3-di(per)fluoroalkyl-2-iodo-*n*-propyl)-1,2,3-triazole-4-carboxamides

Ivanna Danyliuk^{a*}, Sergiy Kemsnyi^a, Lesya Saliyeva^b, Nataliia Slyvka^b, Dmytro Mel'nyk^c, Oksana Mel'nyk^c, Victor Dorokhov^a and Mykhailo Vovk^a

^aInstitute of Organic Chemistry, National Academy of Sciences of Ukraine, 5 Academician Kukhar Str., Kyiv 02660, Ukraine

^bLesya Ukrainka Volyn National University, 13 Voli Avenue, Lutsk 43025, Ukraine

^cIvano-Frankivsk National Medical University, 2 Halytska St., Ivano-Frankivsk 76000, Ukraine

CHRONICLE

Article history:

Received October 10, 2024

Received in revised form

October 30, 2024

Accepted December 20, 2024

Available online

December 20, 2024

Keywords:

1,2,3-Triazole-4-carboxamides

Iododi(per)fluoroalkylation

DPPH

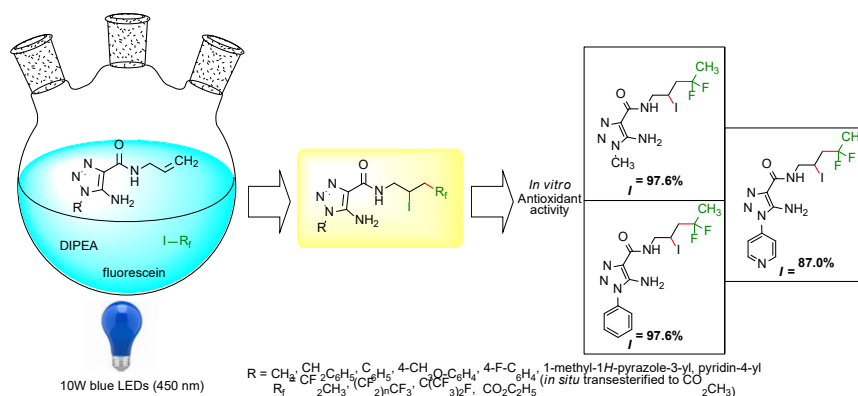
Antioxidant activity

Docking studies

ABSTRACT

Antioxidant activity of a series of previously described 5-amino-*N*-(iododi(per)fluoroalkyl)-1*H*-1,2,3-triazole-4-carboxamides **3a-r**, their synthetic precursors 5-amino-*N*-allyl-1,2,3-triazole-4-carboxamides **1a-g**, and their deamination products *N*-(3-di(per)fluoroalkyl-2-iodo-*n*-propyl)-1,2,3-triazole-4-carboxamides **4a-e** was investigated *in vitro* using DPPH test and ascorbic acid as a standard reference. It was established that compounds **3a-r** inhibit DPPH free radicals in moderate to high values (50.9–97.6%). The effect of substituents in the position 1 of the 1,2,3-triazole nucleus, fluoroalkyl groups and amino groups on the level of antioxidant activity was studied in detail. Reactivity and electrostatic surface potential were evaluated for the most active carboxamides **3a,g,r** using the DFT method, and molecular docking was studied in the NADPH oxidase protein model.

© 2025 by the authors; licensee Growing Science, Canada.



Graphical Abstract

1. Introduction

Among the five-membered nitrogen-containing heteroaromatic systems, 1,2,3-triazoles are representatives of structures with powerful synthetic,¹⁻⁶ medical-biological,⁷⁻¹⁴ and materials science^{15,16} potential. It is important that almost all biologically active derivatives usually contain various functional groups in addition to the pharmacophoric 1,2,3-triazole scaffold. The importance of 1,2,3-triazole carboxamides is also worth noting, which are the basis of a number of synthetic drugs, including the anticonvulsant drug Rufinamide, the antiproliferative drug Carboxyamidotriazole (CAI) and the

* Corresponding author Tel.: +380-68-729-20-47
E-mail address ivannayu@ukr.net (I. Danyliuk)

antiretroviral drug *tert*-butyldimethylsilyl-spiroaminoxathioledioxide (TSAO) (See **Fig. 1**). Of these, CAI deserves special attention due to antitumor, antiangiogenic and antimetastatic properties and is structurally an analogue of anthranilic acid amide, the derivatives of which are noted for their wide therapeutic potential.¹⁷

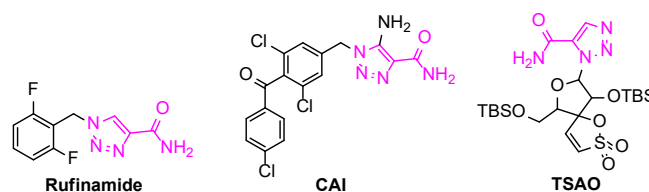


Fig. 1. Pharmaceutical preparations based on the 1,2,3-triazole carboxamide

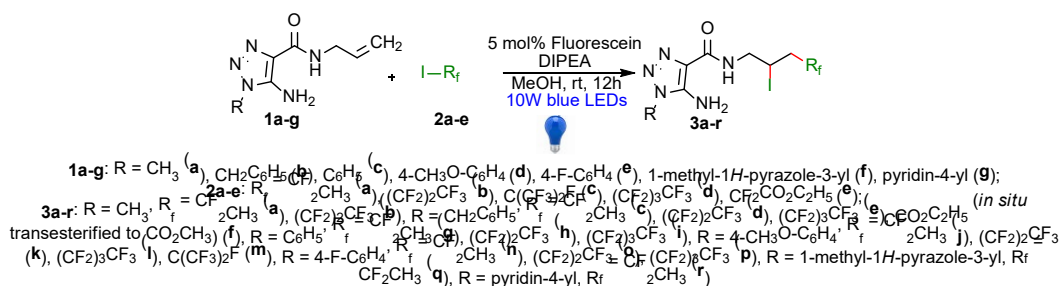
Generally, 5-amino-1,2,3-triazole-4-carboxamide derivatives are very interesting research objects in medicinal and pharmaceutical chemistry due to their diverse spectrum of pharmacological activity. It is known that they exhibit inhibitory activity against bacterial LexA repressor-protease,¹⁸ vascular endothelial growth factor receptors I and II (VEGF 1 and 2),¹⁹ block mitochondrial complex I, which makes them promising for anticancer and radiosensitizing therapy,²⁰ and also act as selective release inhibitors of interleukin-1 β .²¹ They also show promising antimicrobial properties by inhibiting the SOS-dependent response of bacteria,^{22,23} as well as activity against varicella-zoster virus and cytomegalovirus,²⁴ and are potentially promising for the treatment of Chagas disease. It was experimentally proven that the bioactivity of the triazole core is enhanced by amino group in position 5 which can form an intramolecular hydrogen bond with the amide carbonyl group stabilizing the bioactive conformation, or participate in specific interactions with molecular targets.²⁵ The introduction of fluorine atoms or fluoroalkyl groups into the side chain of 1,2,3-triazole in combination with iodine atoms is also important, since such substituents significantly affect key pharmacological parameters. They improve membrane permeability, increase metabolic stability, lipophilicity and affinity to biological targets. As a rule, this leads to an increase in the biological and pharmacological effectiveness of potential drugs.²⁶⁻³¹

One of the priority directions of modern medical and pharmaceutical chemistry is the search for compounds with antioxidant properties to effectively combat oxidative stress.³²⁻³⁴ Oxidative stress occurs due to an imbalance between the formation and accumulation of reactive oxygen species in cells and tissues. This plays a critical role in the development of a variety of chronic and degenerative diseases such as aging, cancer, cataracts, autoimmune disorders, rheumatoid arthritis, cardiovascular and neurodegenerative diseases. The human body is able to combat oxidative stress due to the action of antioxidants which it can synthesize naturally or obtain from the outside through food products and supplements. At the same time, endogenous defense systems are insufficient without exogenous antioxidants so the demand for external antioxidants to prevent oxidative stress is constantly increasing.^{35,36} In the context of the aforementioned, the study of 5-amino-1,2,3-triazole-4-carboxamide derivatives represents a rather interesting perspective. These compounds are characterized by structural flexibility which enables their easy modification with various functional groups, significantly changing their biological properties. The introduction of fluorine-containing groups, iodine atoms, variable substituents in position 1 of the triazole nucleus and the effect of an amino group in position 5 can significantly vary the activity of 1,2,3-triazole-4-carboxamide derivatives which opens new horizons for the development of innovative therapeutic agents.

2. Results and Discussion

2.1 Chemistry and antioxidant activity

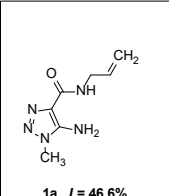
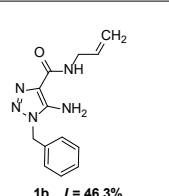
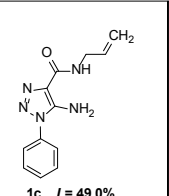
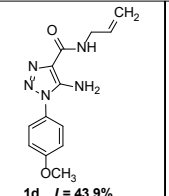
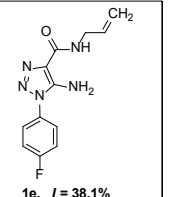
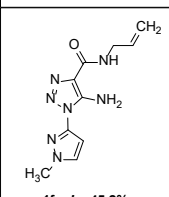
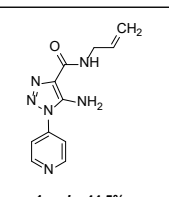
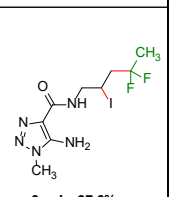
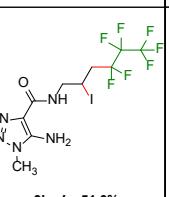
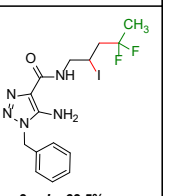
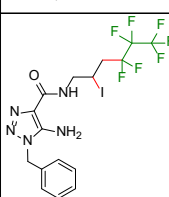
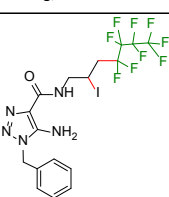
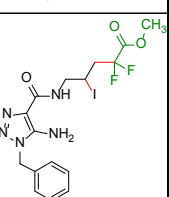
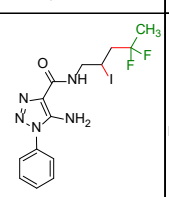
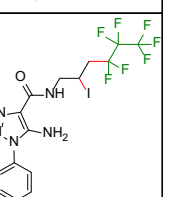
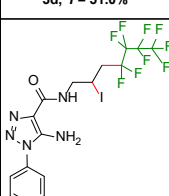
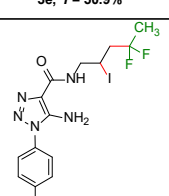
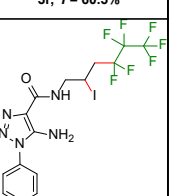
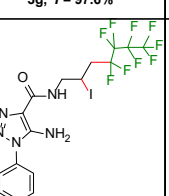
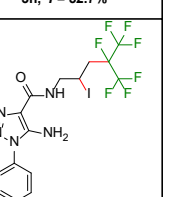
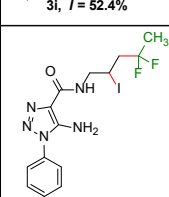
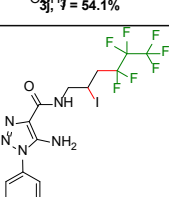
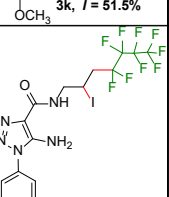
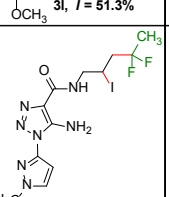
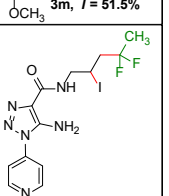
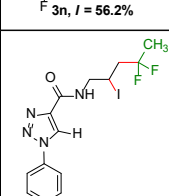
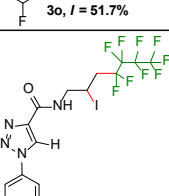
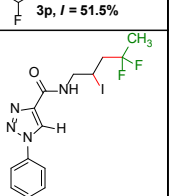
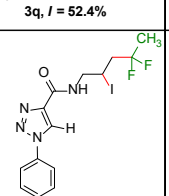
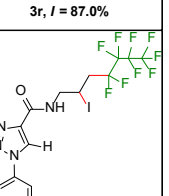
The creation of a focused library of 5-amino-*N*-(iodo(per)fluoroalkyl-functionalized)-1*H*-1,2,3-triazole-4-carboxamides for further medical and biological research used the previously described organophotocatalytic method of defunctionalization of the double bond of derivatives 5-amino-*N*-allyl-1,2,3-triazole-4-carboxamides with commercially available di(per)fluoroalkyl iodides in the presence of the environmentally and economically attractive photocatalyst fluorescein.³⁷



Scheme 1. Synthesis of 5-amino-*N*-(3-di(per)fluoroalkyl-2-iodo-*n*-propyl)-1,2,3-triazole-4-carboxamides **3a-r**

Variations of 5-amino-*N*-allyl-1,2,3-triazole-4-carboxamides **1a-g** and fluoroalkyl iodides 1,1-difluoroethyl iodide **2a**, *n*-perfluoropropyl iodide **2b**, perfluoroisopropyl iodide **2c**, *n*-perfluorobutyl iodide **2d** and ethyl difluoroiodoacetate **2e** allowed us to obtain a series of pharmacologically attractive compounds of type **3** and to investigate the effect of substituents in the carboxamide fragment on the antioxidant activity (See **Scheme 1**). Obtained compounds (See **Table 1**) were tested *in vitro* for their ability to inhibit 2,2-diphenyl-1-picrylhydrazyl (DPPH) radicals at a concentration of 5 mM (methanol solution, measurement after 60 min). Ascorbic acid was used as a reference compound. The results of experiments showed that 5-amino-*N*-(iodo(per)fluoroalkyl functionalized)-1*H*-1,2,3-triazole-4-carboxamides **3a-r** absorb from 50.9 to 97.6% of the formed radicals. The most pronounced antioxidant effect was observed for 5-amino-*N*-(4,4-difluoro-2-iodopentyl)-1-methyl-1*H*-1,2,3-triazole-4-carboxamide **3a** and 5-amino-*N*-(4,4-difluoro-2-iodopentyl)-1-phenyl-1*H*-1,2,3-triazole-4-carboxamide **3g** where inhibition was 97.6%. A somewhat lower level of DPPH radical inhibition was shown by 5-amino-*N*-(4,4-difluoro-2-iodopentyl)-1-(pyridin-4-yl)-1*H*-1,2,3-triazole-4-carboxamide **3r** ($I = 87.0\%$). Analysis of the structure–activity dependence confirmed the positive effect of iodo(per)fluoroalkyl substituents, in particular 4,4-difluoro-2-iodo group, on the antioxidant activity of the studied compounds. For comparison, the starting 5-amino-*N*-allyl-1,2,3-triazole-4-carboxamides **1a-g** absorb only 38.1–46.6% of DPPH radicals, whereas their difunctionalized derivatives **3a-r** showed a much higher level of inhibition, reaching 50.9–97.6%. In addition, it was found that the nature of perfluoroalkyl groups also plays an important role, specifically that the lengthening of the fluorinated chain caused a decrease in antioxidant activity (See **Table 1**, **Figs. 2,3**).

Table 1. Antioxidant activity 1,2,3-triazole-4-carboxamides **1a-g**, **3a-r** and **4a-e**

 1a , $I = 46.6\%$	 1b , $I = 46.3\%$	 1c , $I = 49.0\%$	 1d , $I = 43.9\%$	 1e , $I = 38.1\%$
 1f , $I = 45.2\%$	 1g , $I = 44.5\%$	 3a , $I = 97.6\%$	 3b , $I = 51.0\%$	 3c , $I = 63.5\%$
 3d , $I = 51.0\%$	 3e , $I = 50.9\%$	 3f , $I = 60.5\%$	 3g , $I = 97.6\%$	 3h , $I = 52.7\%$
 3i , $I = 52.4\%$	 3j , $I = 54.1\%$	 3k , $I = 51.5\%$	 3l , $I = 51.3\%$	 3m , $I = 51.5\%$
 3n , $I = 56.2\%$	 3o , $I = 51.7\%$	 3p , $I = 51.5\%$	 3q , $I = 52.4\%$	 3r , $I = 87.0\%$
 4a , $I = 59.0\%$	 4b , $I = 49.1\%$	 4c , $I = 54.1\%$	 4d , $I = 56.2\%$	 4e , $I = 53.8\%$

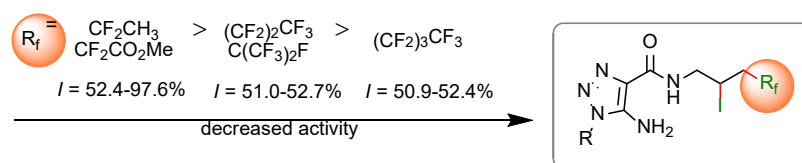
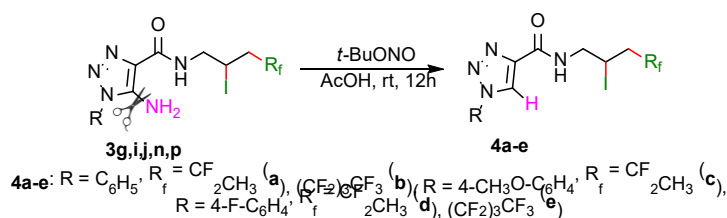


Fig. 2. Structure-anti-radical activity relationships of 5-amino-*N*-(3-di(per)fluoroalkyl-2-iodo-*n*-propyl)-1,2,3-triazole-4-carboxamides **3a-r**.

Substituents in position 1 of the 1,2,3-triazole core do not show such a systematic dependence. For instance, a significant increase in antioxidant activity is observed for 5-amino-*N*-(3-difluoroalkyl-2-iodo-*n*-propyl)-1,2,3-triazole-4-carboxamides **3a,c,g,n,r** with substituents R = CH₃, CH₂C₆H₅, C₆H₅, 4-F-C₆H₄ and pyridin-4-yl (*I* = 56.2–97.6%). On the contrary, the introduction of substituents R = 4-CH₃O-C₆H₄ and 1-methyl-1*H*-pyrazole-3-yl led to slightly lower rates of inhibition of DPPH radicals (52.4–54.1%, respectively). To study the effect of the 5-amino group on the antioxidant activity, a series of *N*-(3-di(per)fluoroalkyl-2-iodo-*n*-propyl)-1,2,3-triazole-4-carboxamides **4a-e** was synthesized by the deamination reaction of compounds **3g,i,j,n,p** under the action of *tert*-butyl nitrite in acetic acid (See **Scheme 2**). The study shows that the removal of the amino group in the position 5 of the triazole nucleus leads to some decrease in antioxidant activity (*I* = 49.1–59.0%) (See **Table 1**, **Fig. 3**). Although the decrease in activity is not substantial, the difference is worth noting, as it indicates that the 5-amino group plays a significant role in the effective inhibition of free radicals, which is evidence of its key importance for optimizing the antioxidant properties of the studied molecules.



Scheme 2. Synthesis of *N*-(3-di(per)fluoroalkyl-2-iodo-*n*-propyl)-1,2,3-triazole-4-carboxamides **4a-e**

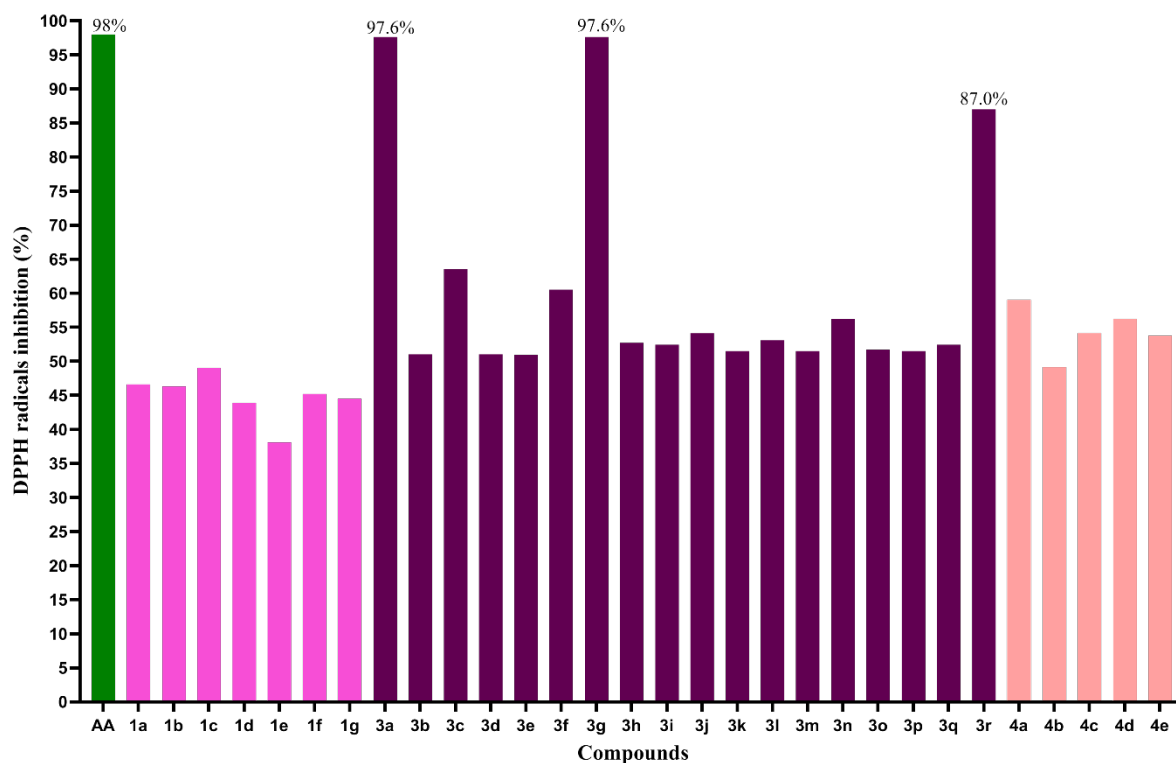
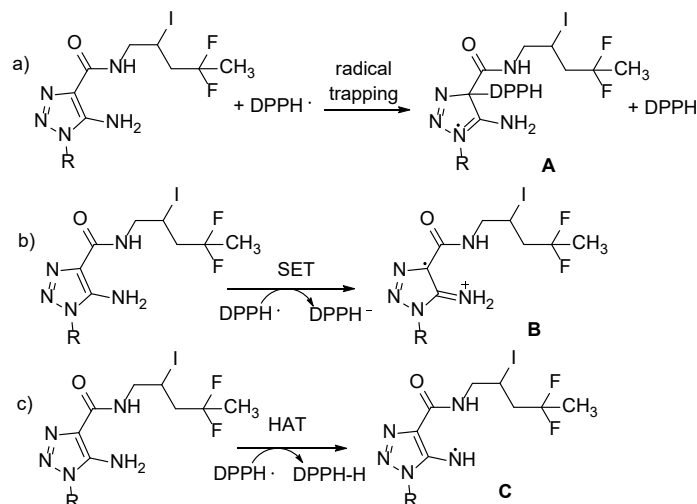


Fig. 3. The inhibition of DPPH radicals by the 1,2,3-triazole derivatives **1a-g**, **3a-r**, **4a-e** at 5 mM concentration.

Considering the recent study³⁸ which allows for the possibility of several directions of antioxidant action of organic compounds, we studied possible options for inhibiting DPPH free radicals for the most active 5-amino-*N*-(3-

di(per)fluoroalkyl-2-iodo-n-propyl)-1,2,3-triazole-4-carboxamides **3a,g,r** (See **Scheme 3**). They include the mechanism of spin capture, which results in the formation of spin adduct **A** with DPPH (pathway a); sequential electron transfer (SET) (pathway b) and/or hydrogen atom transfer (HAT) (pathway c).



Scheme 3. Probable pathways of DPPH inhibition by compounds **3a,g,r**

2.2. Structure and reactivity analysis by the method of DFT-calculation

The structures of compounds with antioxidant activity **3a,g,r** were optimized using Gaussian 09 software,³⁹ and the results were visualized using GaussView 5.0.8. The geometry of all studied structures was optimized using the density functional B3LYP method. The relativistic effective core potential basis set of Lanl2dz was used on the iodine atom, and the 6-311++G(d,p) was used on the other atoms.^{40,41}

The reactivity parameters of the **3a,g,r** molecules, such as ionization potential (IP), electron affinity (EA), chemical hardness (η), global electrophilicity power (ω)⁴²⁻⁴⁴ and nucleophilic (N) power in scale that referred to tetracyanoethylene (TCE) taken as a reference because it presents the lowest HOMO energy in a large series of molecules already considered.⁴⁵

$$\begin{aligned} \text{IP} &= -E_{\text{HOMO}} \\ \text{EA} &= -E_{\text{LUMO}} \\ \eta &= \text{IP} - \text{EA} \\ \mu &= -0,5(\text{IP} + \text{EA}) \\ \omega &= \mu^2/2\eta \\ \text{N} &= \text{IP}(\text{TCE}) - \text{IP}(\text{Nu}) \end{aligned}$$

According to the B3LYP/6-311++G(d,p)-based (the relativistic effective core potential basis set of Lanl2dz was used on iodine atom) DFT-simulation of molecular structures **3a,g,r** in vacuum (See **Fig. 4**), the angle between the aryl substituent and the triazole fragment is about 40°, and the angle N4–N3–C29–C30 is; 41.6° (**3g**) and 33.9° (**3r**), correspondingly.

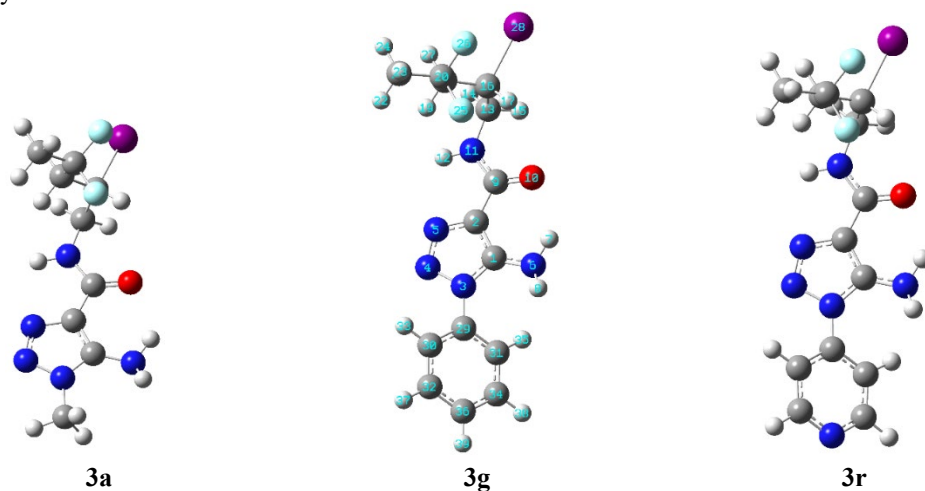


Fig. 4. DFT-optimized structure of the compounds **3a,g,r**

The energy of the frontier MOs depends on the electron donating power of the substituent in the triazole ring. Thus, the highest energy of the frontier MOs is found in compound **3a** with a methyl group, and the lowest in the compound **3r** with a pyridin group. The calculated values of HOMO, LUMO, and other electronic parameters are shown in **Table 2**. The calculated HOMO energy show that they increase in the order $3r < 3g = 3a$, and compounds **3a** and **3g** is better electron donors. This is also proved by higher value of the nucleophilic (N) powers.

Table 2. Calculated energy of the frontier MOs, electron affinity (EA), ionization potential (IP), chemical hardness (η), chemical potential (μ), global electrophilicity power (ω) and nucleophilic (N) powers.

	3a	3g	3r
LUMO, eV	-1.23	-1.46	-1.99
HOMO, eV	-6.60	-6.60	-6.86
EA, eV	1.23	1.46	1.99
IP, eV	6.60	6.60	6.86
η , eV	5.37	5.13	4.86
μ , eV	-3.91	-4.03	-4.43
ω , eV	1.43	1.58	2.01
N, eV	2.89	2.89	2.63

The molecular electrostatic surface potential (MESP) is an important factor for describing the active sites of ligands.^{46,47} It was calculated for the molecules of compounds **3a,g,r** using optimized structures with the B3LYP/6-311++G(d,p) basis (Lan12dz was used on iodine atom) for studying nucleophilic and electrophilic surface spots. All compounds have a negatively charged spots (electrophilic center) located near the nitrogen atom at position 2,3 of the triazole cycle, carbonyl group and iodine atom (See **Fig. 5**). The most positively charged surface area is near both amino groups.

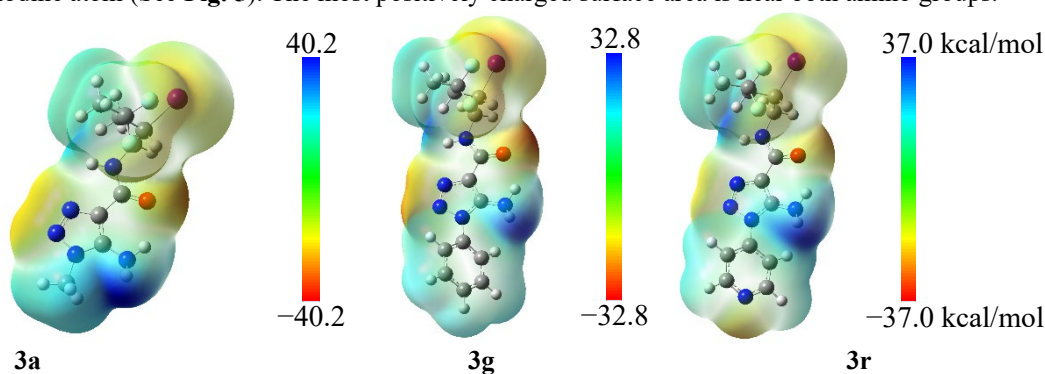


Fig. 5. Calculated MESP for the molecules of **3a,g,r**

In our case DPPH is model radical, **Scheme 3** summarizes possible reaction mechanisms that could take place between DPPH and the compound **3a**. In a typical DPPH assay, conjugated compounds are therefore expected to quench DPPH free radicals via a spin trapping mechanism following pathway (a), giving rise to spin adduct **A**. But this process is unlikely due to significant steric interferences. That is why the formation of cationic radical **B** by the SET process seems more likely (**Scheme 3**, pathway b). The analysis of its spin density (s) shows that it is mainly focused on the carbon atom in the position 4 triazole cycle ($s(C2) = 0.2845$) and on the iodine atom ($s(I) = 0.325$), and the total spin density from MESP (See **Fig. 6b**) indicates the location of the unpaired electron above the carbon atom in the position 4 triazole cycle. In addition, the electrostatic potential of cation-radical **B** (See **Fig. 6a**) indicates the presence of a positively charged site near the nitrogen atoms both amino groups and in position 1 of triazole ring. The biggest positive charge is on the ammino group of triazole ring which leads to the conclusion main structure of delocalization positive charge of cation radical shown in **Scheme 2**, pathway b.

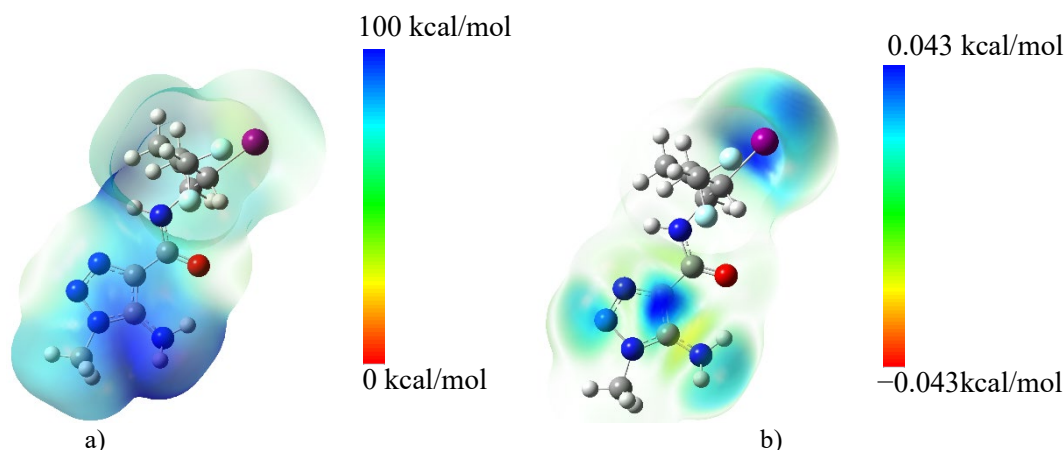


Fig. 6. Calculated positive MESP (a) and total spin density from MESP (b) of cation radical **B**.

2.3. Docking studies

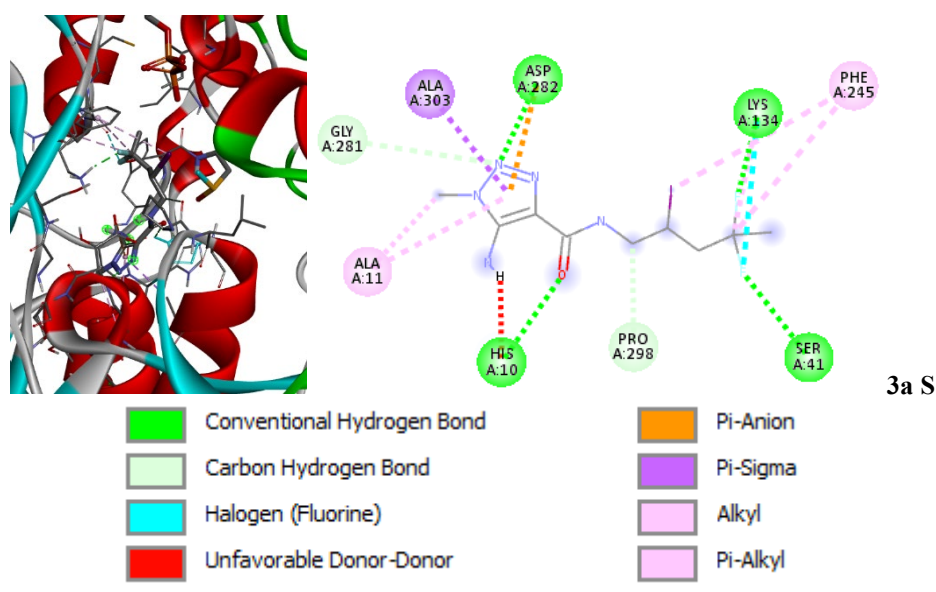
The molecular docking study was performed by the Autodoc Vina software⁴⁸ using previously optimized structures and its R enantiomers. The crystal structure of NADPH oxidase which is associated with antioxidant mechanisms^{40,49} was downloaded from the Protein Data Bank (PDB ID: 2CDU), water molecules were removed, polar hydrogen atoms were added, and the Gasteiger charge was added. A center of the ligand docking cavity (2.4, 2.1, -1.0) was determined using BIOVIA Discovery Studio Visualizer v21.1 and the cavity dimension was 42; 24; 50. Binding was visualized using BIOVIA Discovery Studio Visualizer v21.1.

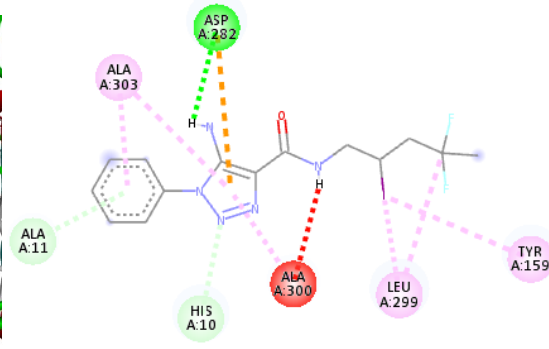
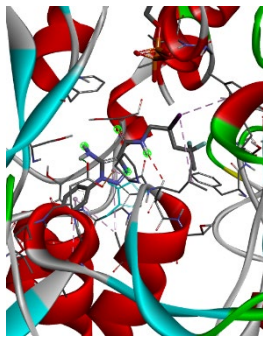
According to the molecular docking simulation, 9 positions were found with the corresponding ligand-protein affinity for every ligand. Docking of the corresponding R enantiomers was also carried out. Compounds **3g** and **3r** showed a higher binding energy in the active site of the protein, especially their R-stereoisomer (See **Table 3**).

Table 3. Ligand-protein interaction of compounds **3a,g,r** with NADPH oxidase (PDB ID: 2CDU).

Parameter	1S	2S	3S	1R	2R	3R
Best binding energy to protein, kcal/mol	-7.4	-8.6	-8.4	-7.2	-8.8	-8.6
Hydrogen bonds	His10 (2.61Å), Asp282 (2.30Å), Lys134 (2.30Å), Ser41 (2.58Å),	Asp282 (2.23Å),	-	His10 (2.61Å), Asp282 (2.30Å), Lys134 (2.38Å),	Thr9 (2.16Å), Cys8 (2.66Å), Thr113 (2.46Å, 2.64),	His10 (2.66Å), Asp282 (2.30Å),
Carbon hydrogen bond	Gly281	Ala11, His10	Ala11, His10			Ala11
Hydrophobic interactions	Ala11, Ala303, Phe245	Ala303, Leu299, Tyr159	Ala303, Leu299, Tyr159	Leu299, Phe245	Ala11, Val6, Met33, Ala303, Leu251, Tyr159	Ala300, Ala303, Leu299, Tyr159
π -anion interaction	Asp282	Asp282	Asp282			
Halogen (Fluorine)			Phe425			Phe425
Unfavorable Donor-Donor	His10	Ala300	Ala300	-	-	-

The ligand-protein interactions for compounds **3a,g,r** visualized in BIOVIA Discovery Studio Visualizer are shown in **Fig. 7**. All compounds in the active site were bound by both hydrogen bonds and nonpolar interactions. The best binding of all S isomers contained an unfavorable interaction between the two hydrogen donor groups, due to which they had slightly lower binding energies.

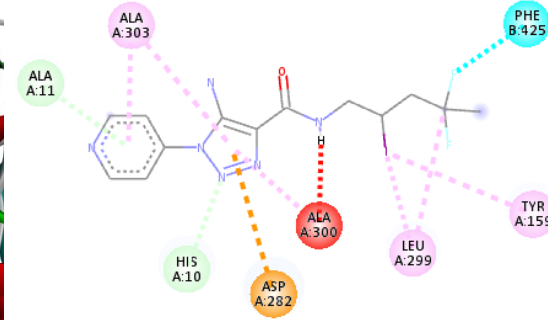
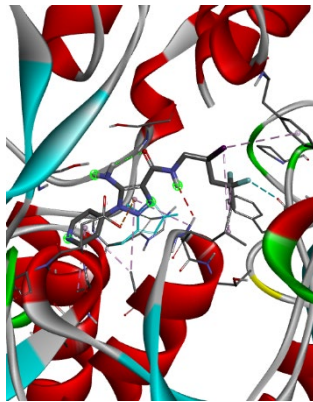




3g S

- Conventional Hydrogen Bond
- Carbon Hydrogen Bond
- Unfavorable Donor-Donor
- Pi-Anion

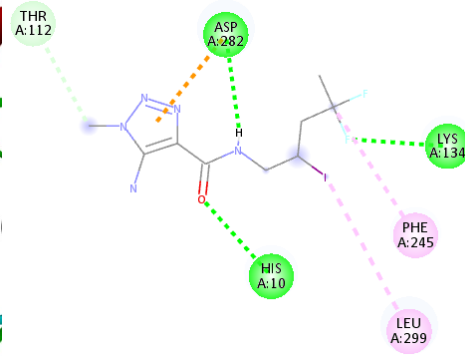
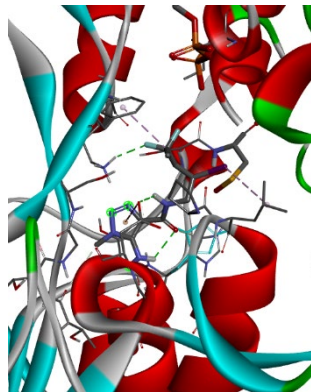
- Pi-Donor Hydrogen Bond
- Alkyl
- Pi-Alkyl



3r S

- Carbon Hydrogen Bond
- Halogen (Fluorine)
- Unfavorable Donor-Donor
- Pi-Anion

- Pi-Donor Hydrogen Bond
- Alkyl
- Pi-Alkyl



3a R

- Conventional Hydrogen Bond
- Carbon Hydrogen Bond
- Pi-Anion

- Alkyl
- Pi-Alkyl

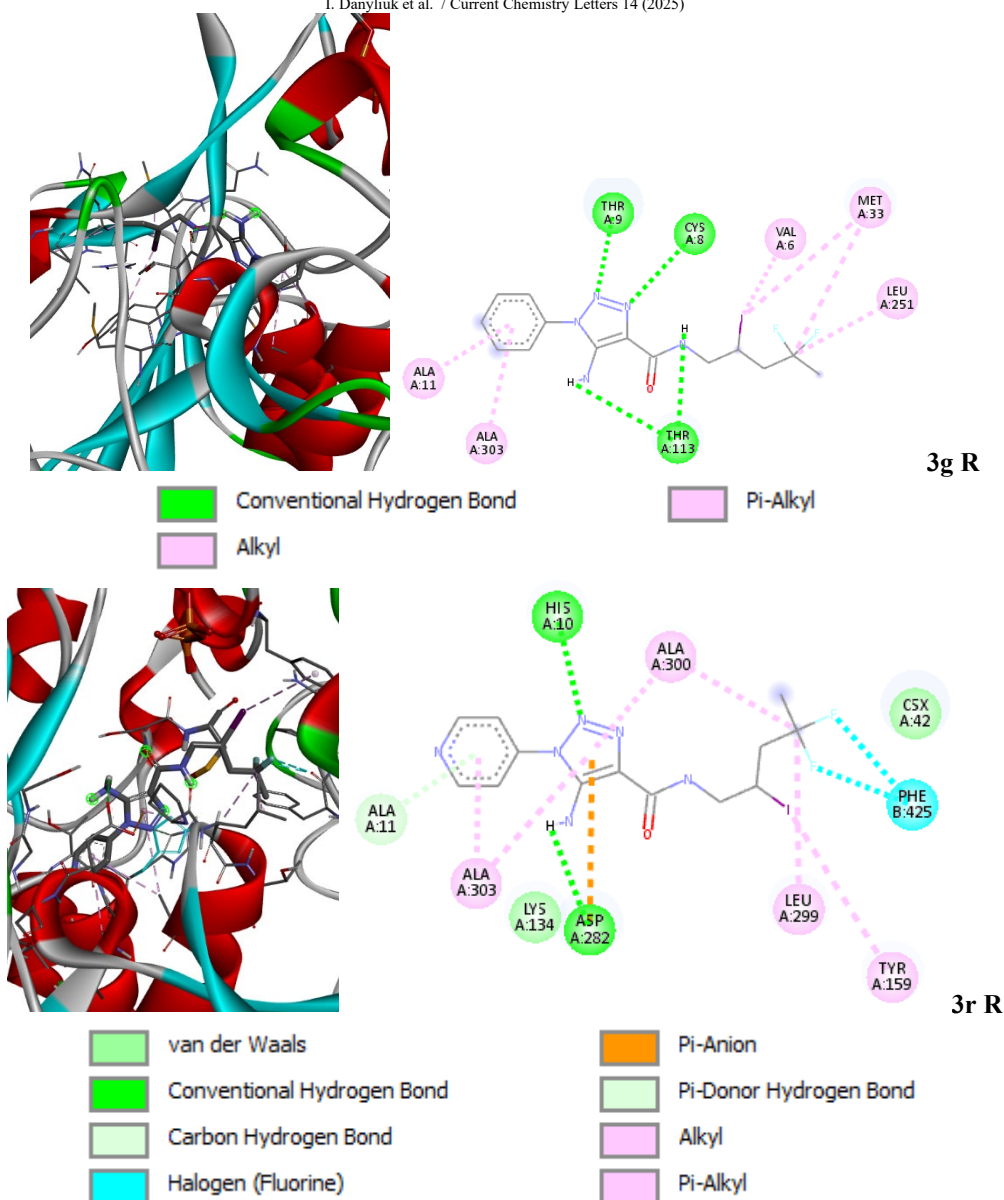


Fig. 7. 3D (left) and 2D (right) interactions of compounds **3a,g,r** inside the active site of the protein.

3. Conclusions

Performed experimental studies convincingly prove that 5-amino-*N*-(iodo(per)fluoroalkyl functionalized)-1*H*-1,2,3-triazole-4-carboxamides are potential antioxidant agents characterized by the ability to inhibit free radicals in the conditions of the experiment with DPPH in the range of 50.9–97.6%. It was found that the substituents in position 1 of the 1,2,3-triazole nucleus, fluoroalkyl groups and the amino group play an important role in determining the level of antioxidant activity of these compounds. A number of compounds with top antiradical activity were identified, which are of interest for advanced pharmacological studies and design of potential synthetic antioxidants. Their structure, reactivity, and MESP were analyzed by DFT calculations, while molecular docking was used to estimate their affinity for NADPH oxidase.

Acknowledgements

We are grateful to Enamine Ltd (Kyiv, Ukraine) for support.

4. Experimental

4.1. Materials and Methods

¹H-NMR spectra were acquired on a Varian Mercury 300 spectrometer (300 MHz) in CDCl₃ solution with TMS as an internal standard. ¹³C, NMR spectra were acquired on a Varian Mercury 300 spectrometer (76 MHz) in CDCl₃ solution (for compound **4b**), Bruker AVANCE DRX 500 spectrometer (125 MHz) in CDCl₃ solution (for compound **4c**), and a Agilent

600MHz spectrometer (150 MHz) in CDCl₃ solution (for compounds **4a,d,e**) with TMS as an internal standard. ¹⁹F, NMR spectra were acquired on a Bruker AC200 spectrometer (188 MHz) in CDCl₃ solution. Melting points were determined on a Kofler bench and are uncorrected. Mass spectra were recorded on an Agilent LC/MSD SL mass spectrometer; column: Zorbax SB-C18, 4.6 × 15 mm, 1.8 μm (PN 82 (c)75-932); DMSO solvent, atmospheric pressure electrospray ionization. Reagents and solvents were purchased from UkrOrgSyntez Ltd. IR spectra were recorded on a Vertex-70 spectrometer from KBr pellets.

4.2. General procedure

General procedure for the synthesis of compounds 4a-e. A solution of 5-amino-*N*-(3-di(per)fluoroalkyl-2-iodo-*n*-propyl)-1,2,3-triazole-4-carboxamides **3a-r** (1 mmol) in acetic acid (AcOH) (5 mL) was added dropwise over 15 min to a solution of *t*-BuONO (1.5 mmol) in AcOH (5 mL) at room temperature for 12 h. The solvent was evaporated, water was added (20 mL) and the mixture was extracted with dichloromethane (DCM) (3 × 15 mL). The organic layers were collected, dried over anhydrous MgSO₄ and filtered, the solvent was removed and the residue was purified by column chromatography on silica gel (with a 35:1 chloroform-methanol mixture as an eluent).

4.3. Physical and Spectral Data

4.3.1. *N*-(4,4-Difluoro-2-iodopentyl)-1-phenyl-1*H*-1,2,3-triazole-4-carboxamide (4a). White solid, mp 117-119°C; yield 81%. ¹H-NMR (302 MHz, CDCl₃): δ 1.69 (t, 3H, *J* = 18.4 Hz, CF₂CH₃), 2.62-2.75 (m, 2H, CH₂CF₂), 3.73-3.82 (m, 1H, CH₂NH), 3.96-4.04 (m, 1H, CH₂NH), 4.44-4.52 (m, 1H, CH-I), 7.50-7.65 (m, 4H, Ar-H + NH), 7.74-7.76 (m, 2H, Ar-H), 8.51 (m, 1H, 1H_{triazole}). ¹³C-NMR (151 MHz, CDCl₃): δ CF₂ signals are not assigned, 22.17, 23.88 (t, *J* = 27.2 Hz), 46.23 (t, *J* = 25.7 Hz), 47.30, 120.75, 123.68, 129.50, 129.97, 136.50, 143.33, 159.91. ¹⁹F-NMR (188 MHz, CDCl₃): δ - 87.75 to - 87.99 (m, 1F), - 89.77 to - 90.04 (m, 1F). IR (KBr, cm⁻¹): 1662 (C=O), 3303-3373 (N-H). HRMS-ESI (m/z): [M+H]⁺ calcd for C₁₄H₁₆F₂IN₄O⁺, 421.0331; found 421.0332.

4.3.2. *N*-(4,4,5,5,6,6,7,7,7-Nonafluoro-2-iodoheptyl)-1-phenyl-1*H*-1,2,3-triazole-4-carboxamide (4b). White solid, mp 165-167°C; yield 90%. ¹H-NMR (302 MHz, CDCl₃): δ 2.81-2.99 (m, 2H, CH₂CF₂), 3.80-3.89 (m, 1H, CH₂NH), 3.94-4.04 (m, 1H, CH₂NH), 4.49-4.59 (m, 1H, CH-I), 7.48-7.60 (m, 3H, Ar-H + NH), 7.71-7.77 (m, 3H, Ar-H), 8.54 (m, 1H, 1H_{triazole}). ¹³C-NMR (76 MHz, CDCl₃): δ CF₃(CF₂)₃ signals are not assigned, 17.18, 39.01 (t, *J* = 21.3 Hz), 47.39, 120.86, 123.90, 129.68, 130.10, 136.55, 143.20, 160.12. ¹⁹F-NMR (188 MHz, CDCl₃): δ - 80.75 to - 80.84 (m, 3F), - 112.82 to - 113.51 (m, 2F), - 124.11 to - 124.28 (m, 2F), - 125.61 to - 125.75 (m, 2F). IR (KBr, cm⁻¹): 1659 (C=O), 3333 (N-H). HRMS-ESI (m/z): [M+H]⁺ calcd for C₁₆H₁₃F₉IN₄O⁺, 574.9985; found 574.9996.

4.3.3. *N*-(4,4-Difluoro-2-iodopentyl)-1-(4-methoxyphenyl)-1*H*-1,2,3-triazole-4-carboxamide (4c). White solid, mp 145-147°C; yield 93%. ¹H-NMR (302 MHz, CDCl₃): δ 1.68 (t, 3H, *J* = 18.1 Hz, CF₂CH₃), 2.62-2.75 (m, 2H, CH₂CF₂), 3.72-3.81 (m, 1H, CH₂NH), 3.88 (s, 3H, OCH₃), 3.94-4.03 (m, 1H, CH₂NH), 4.43-4.52 (m, 1H, CH-I), 7.04 (d, 2H, *J* = 9.1 Hz, Ar-H); 7.63-7.66 (m, 3H, Ar-H + NH), 8.42 (m, 1H, 1H_{triazole}). ¹³C-NMR (126 MHz, CDCl₃): δ 21.66, 23.35 (t, *J* = 27.7 Hz), 45.71 (t, *J* = 25.4 Hz), 46.83, 55.16, 114.47, 121.86, 122.58 (t, *J* = 241.3 Hz, CF₃), 123.25, 129.36, 142.64, 159.53, 159.85. ¹⁹F-NMR (188 MHz, CDCl₃): δ - 86.48 to - 88.03 (m, 1F); - 89.57 to - 91.24 (m, 1F). IR (KBr, cm⁻¹): 1662 (C=O), 3293 (N-H). HRMS-ESI (m/z): [M+H]⁺ calcd for C₁₅H₁₈F₂IN₄O₂⁺, 451.0437; found 451.0440.

4.3.4. *N*-(4,4-Difluoro-2-iodopentyl)-1-(4-fluorophenyl)-1*H*-1,2,3-triazole-4-carboxamide (4d). White solid, mp 133-135°C; yield 85%. ¹H-NMR (302 MHz, CDCl₃): δ 1.69 (t, 3H, *J* = 19.6 Hz, CF₂CH₃), 2.62-2.75 (m, 2H, CH₂CF₂), 3.72-3.82 (m, 1H, CH₂NH), 3.95-4.04 (m, 1H, CH₂NH), 4.44-4.52 (m, 1H, CH-I), 7.24-7.29 (m, 2H, Ar-H), 7.59-7.64 (m, 1H, NH), 7.71-7.76 (m, 2H, Ar-H), 8.47 (m, 1H, 1H_{triazole}). ¹³C-NMR (151 MHz, CDCl₃): δ 22.14, 23.89 (t, *J* = 27.2 Hz), 46.24 (t, *J* = 25.7 Hz), 47.29, 117.00 (d, *J* = 24.2 Hz), 122.81 (d, *J* = 9.1 Hz), 123.12 (t, *J* = 240.8 Hz, CF₃), 123.89, 132.74 (d, *J* = 3.02 Hz), 143.42, 159.81, 162.84 (d, *J* = 250.7 Hz). ¹⁹F-NMR (188 MHz, CDCl₃): δ - 86.50 to - 88.16 (m, 1F); - 89.82 to - 91.40 (m, 1F); - 110.67 (s, 1F). IR (KBr, cm⁻¹): 1660 (C=O), 3309-3355 (N-H). HRMS-ESI (m/z): [M+H]⁺ calcd for C₁₄H₁₅F₃IN₄O⁺, 439.0237; found 439.0239.

4.3.5. 1-(4-Fluorophenyl)-*N*-(4,4,5,5,6,6,7,7,7-nonafluoro-2-iodoheptyl)-1*H*-1,2,3-triazole-4-carboxamide (4e). White solid, mp 158-160°C; yield 87%. ¹H-NMR (302 MHz, CDCl₃): δ 2.83-2.97 (m, 2H, CH₂CF₂), 3.78-3.88 (m, 1H, CH₂NH), 3.94-4.03 (m, 1H, CH₂NH), 4.48-4.57 (m, 1H, CH-I), 7.24-7.30 (m, 2H, Ar-H), 7.63-7.67 (m, 1H, NH), 7.71-7.76 (m, 2H, Ar-H), 8.48 (m, 1H, 1H_{triazole}). ¹³C-NMR (151 MHz, CDCl₃): δ CF₃(CF₂)₃ signals are not assigned, 17.03, 38.94 (t, *J* = 21.1 Hz), 47.29, 117.03 (d, *J* = 24.2 Hz), 122.82 (d, *J* = 9.0 Hz), 123.97, 132.70 (d, *J* = 3.0 Hz), 143.23, 159.89, 162.89 (d, *J* = 250.7 Hz). ¹⁹F-NMR (188 MHz, CDCl₃): δ - 80.86 to - 80.97 (m, 3F); - 110.54 (s, 1F); - 112.89 to - 113.69 (m, 2F); - 124.21 to - 124.44 (m, 2F); - 125.69 to - 125.93 (m, 2F). IR (KBr, cm⁻¹): 1656 (C=O), 3339 (N-H). HRMS-ESI (m/z): [M+H]⁺ calcd for C₁₆H₁₂F₁₀IN₄O⁺, 592.9890; found 592.9893.

4.4. Antioxidant activity (DPPH assay)

Antioxidant activity of the synthesized compounds was assessed using the 2,2-diphenyl-1-picrylhydrazyl (DPPH) radical inhibition assay.⁵⁰ 1 ml of DPPH solution (8 mg/100 ml) was added to solutions of the tested compounds and ascorbic acid in methanol as a standard and left at room temperature in a dark place for 1 hour. The amount of absorption of radicals was determined at 517 nm relative to the standard on a UV-1800 spectrophotometer (Shimadzu, Japan). Each sample was analyzed in triplicate. The percentage of inhibition was calculated relative to the blank sample:

$$I\% = \frac{(A_{\text{blank}} - (A_{\text{sample+DPPH}} - A_{\text{sample}}))}{A_{\text{blank}}} \cdot 100\%$$

where A_{blank} is the absorbance of the control reaction (includes all reagents except the test compounds); $A_{\text{sample+DPPH}}$ is the absorbance of the test compounds after 60 min incubation with DPPH solution; A_{sample} is the absorbance of the test compounds without DPPH solution.

For details, please see Supporting Information available.

References

1. Vala D.P., Vala R.M., and Petel H.M. (2022) Versatile Synthetic Platform for 1,2,3-Triazole Chemistry. *ACS Omega*, 7 (42) 36945-36987 (<https://doi.org/10.1021/acsomega.2c04883>).
2. Motornov V., and Beier P. (2023) NH-1,2,3-Triazoles as Versatile Building Blocks in Denitrogenative Transformations. *RSC Adv.*, 13 (49) 34646-34653 (<https://doi.org/10.1039/D3RA06045D>).
3. Shiri P., Amani A.M., and Mayer-Gall T. (2021) A Recent Overview on the Synthesis of 1,4,5-Trisubstituted 1,2,3-triazoles. *Beilstein J. Org. Chem.*, 17 1600-1628 (<https://doi.org/10.3762/bjoc.17.114>).
4. Reddy G.S., Anebouselvy K., and Ramachary D.B. (2020) [3+2]-Cycloaddition for Fully Decorated Vinyl-1,2,3-Triazoles: Design, Synthesis and Applications. *Chem. Asian. J.*, 15 (19) 2960-2983 (<https://doi.org/10.1002/asia.202000731>).
5. Agouram N., El Hadrami E.M., and Bentama A. (2021) 1,2,3-Triazoles as Biomimetics in Peptide Science. *Molecules*, 26 (10) 2937 (<https://doi.org/10.3390/molecules26102937>).
6. Li W., and Zhang J. (2020). Synthesis of Heterocycles through Denitrogenative Cyclization of Triazoles and Benzotriazoles. *Chemistry*, 26 (52) 11931–11945 (<https://doi.org/10.1002/chem.202000674>).
7. Slavova K.I., Todorov L.T., Belskaya N.P., Palafox M.A., and Kostova I.P. (2020) Developments in the Application of 1,2,3-Triazoles in Cancer Treatment. *Recent Pat Anticancer Drug Discov.*, 15 (2) 92-112 (<https://doi.org/10.2174/1574892815666200717164457>).
8. Forezi L.S.M., Lima C.G.S., Amaral A.A.P., Ferreira P.G., Souza M.C.B.V., Cunha A.C., da Silva F.C., and Ferreira V.F. (2021) Bioactive 1,2,3-Triazoles: An Account on their Synthesis, Structural Diversity and Biological Applications. *The Chemical Record*, 21 (10) 2782-2807 (<https://doi.org/10.1002/tcr.202000185>).
9. Poonia N., Kumar A., Kumar V., Yadav M., and Lal, K. (2021) Recent Progress in 1H-1,2,3-triazoles as Potential Antifungal Agents. *Curr. Top. Med. Chem.*, 21 (23) 2109-2133 (<https://doi.org/10.2174/1568026621666210913122828>).
10. Alam M.M. (2022) 1,2,3-Triazole hybrids as anticancer agents: A review. *Arch Pharm.*, 355 (1) e2100158 (<https://doi.org/10.1002/ardp.202100158>).
11. Ravindar L., Hasbullah S.A., Rakesh K.P., and Hassan, N.I. (2023) Triazole Hybrid Compounds: A new Frontier in Malaria Treatment. *Eur. J. Med. Chem.*, 259 115694 (<https://doi.org/10.1016/j.ejmech.2023.115694>).
12. Vaishnani M.J., Bijani S., Rahamathulla M., Baldaniya L., Jain V., Thajudeen K.Y., Ahmed M.M., Farhana S.A., and Pasha I. (2024) Biological Importance and Synthesis of 1,2,3-Triazole Derivatives: a review. *Green Chem. Lett. and Rev.*, 17 (1) (<https://doi.org/10.1080/17518253.2024.2307989>).
13. Marzi M., Farjam M., Kazeminejad Z., Shiroudi A., Kouhpayeh A., Zarenezhad E. (2022) A Recent Overview of 1,2,3-Triazole-Containing Hybrids as Novel Antifungal Agents: Focusing on Synthesis, Mechanism of Action, and Structure-Activity Relationship (SAR). *J. Chem.*, 1 7884316 (<https://doi.org/10.1155/2022/7884316>).
14. Singh A., Singh K., Sharma A., Joshi K., Singh B., Sharma S., Batra K., Kaur K., Singh D., Chadha R., Mohinder P., Bedi S. (2023) 1,2,3-Triazole Derivatives as an Emerging Scaffold for Antifungal Drug Development against *Candida albicans*: A Comprehensive Review. *Chem. Biodiversity.*, 20 (5) e202300024 (<https://doi.org/10.1002/cbdv.202300024>).
15. Hrimla M., Bahsis L., Laamari M.R., Julve M., and Stiriba S.-E. (2022) An Overview on the Performance of 1,2,3-Triazole Derivatives as Corrosion Inhibitors for Metal Surfaces. *Int. J. Mol. Sci.*, 23 (1) 16 (<https://doi.org/10.3390/ijms23010016>).
16. Farooq T. (2021) Triazoles in Material Sciences. *Advances in Triazole Chemistry*, 223-244 (<https://doi.org/10.1016/B978-0-12-817113-4.00002-0>).
17. Marinova P., and Hristov M. (2023) Synthesis and Biological Activity of Novel Complexes with Anthranilic Acid and its Analogues. *Appl. Sci.*, 13 9426 (<https://doi.org/10.3390/app13169426>).

18. Jaramillo A.V.C., Cory M.B., Li A., Kohli R.M., and Wuest W.M. (2022) Exploration of Inhibitors of the Bacterial LexA Repressor-protease. *Bioorg. Med. Chem. Lett.*, 65 128702 (<https://doi.org/10.1016/j.bmcl.2022.128702>).
19. Kiselyov A., Semenova M., and Semenov V.V. (2009) (1,2,3-Triazol-4-yl)benzenamines: Synthesis and Activity Against VEGF receptors 1 and 2. *Bioorg. Med. Chem. Lett.*, 19 (5) 1344-1348 (<https://doi.org/10.1016/j.bmcl.2009.01.046>).
20. Lan J., Cadassou O., Corbet C., Riant O., and Feron O. (2022) Discovery of Mitochondrial Complex I Inhibitors as Anticancer and Radiosensitizer Drugs Based on Compensatory Stimulation of Lactate Release. *Cancers.*, 14 (21) 5454 (<https://doi.org/10.3390/cancers14215454>).
21. Mu R., Zhou Y., Chen L., Wei H., Yu J., Gou W., Ye C., Hou W., Li Y., and Zhu L. (2021) Discovery of Novel Triazole Compounds as Selective IL-1 β Release Inhibitors. *Bioorg. Med. Chem. Lett.*, 53 128415 (<https://doi.org/10.1016/j.bmcl.2021.128415>).
22. Pokhodylo N., Manko N., Finiuk N., Klyuchivska O., Matiychuk V., Obushak M., and Stoiko R. (2021) Primary Discovery of 1-Aryl-5-substituted-1*H*-1,2,3-triazole-4-carboxamides as Promising Antimicrobial Agents. *J. Mol. Struct.*, 1246 131146 (<https://doi.org/10.1016/j.molstruc.2021.131146>).
23. Selwood T., Larsen B.J., Mo C.Y., Culyba M.J., Hostetler Z.M., Kohli R.M., Reitz A.B., and Baugh S.D.P. (2018) Advancement of the 5-Amino-1-(Carbamoylmethyl)-1*H*-1,2,3-Triazole-4-Carboxamide Scaffold to Disarm the Bacterial SOS Response. *Front. Microbiol.* 9 2961 (<https://doi.org/10.3389/fmicb.2018.02961>).
24. Yuan W., Chen X., Liu N., Wen Y., Yang B., Andrei G., Snoeck R., Xiang Y., Wu Y., Jiang Z., Schols D., Zhang Z., and Wu Q. (2019) Synthesis, Anti-Varicella-Zoster Virus and Anti-Cytomegalovirus Activity of 4,5-Disubstituted 1,2,3-(1*H*)-Triazoles. *Medicinal Chemistry.*, 15 (7) 801-812 (<https://doi.org/10.2174/1573406414666181109095239>).
25. Brand S., Ko E.J., Viayna E., Thompson S., Spinks D., Thomas M., Sandberg L., Francisco A.F., Jayawardhana S., Smith V.C., Jansen C., De Rycker M., Thomas J., MacLean L., Osuna-Cabello M., Riley J., Scullion P., Stojanovski L., Simeons F.R.C., Epemolu O., Shishikura Y., Crouch S.D., Bakshi T.S., Nixon C.J., Reid I.H., Hill A.P., Underwood T.Z., Hindley S.J., Robinson S.A., Kelly J.M., Fiandor J.M., Wyatt P.G., Marco M., Miles T.J., Read K.D., and Gilbert I.H. (2017) Discovery and Optimization of 5-Amino-1,2,3-triazole-4-carboxamide Series against *Trypanosoma cruzi*. *J Med Chem.*, 14 60 (17) 7284-7299 (<https://doi.org/10.1021/acs.jmedchem.7b00463>).
26. Usachev B.I. (2018) Chemistry of Fluoroalkyl-substituted 1,2,3-Triazoles. *J. Fluor. Chem.*, 210 6-45 (<https://doi.org/10.1016/j.jfluchem.2018.02.012>).
27. Ullah I., Ilyas M., Omer M., Alamzeb M., Adnan, and Sohail M. (2022) Fluorinated Triazoles as Privileged Potential Candidates in drug Development—focusing on their Biological and Pharmaceutical Properties. *Front. Chem.*, 10 926723 (<https://doi.org/10.3389/fchem.2022.926723>).
28. Ma J-A., and Cahard D. (2004) Asymmetric Fluorination, Trifluoromethylation, and Perfluoroalkylation Reactions. *Chem. Rev.*, 104 6119-6146 (<https://doi.org/10.1021/cr030143e>).
29. Kaiho T. (2015) Iodine Chemistry and Applications, *Wiley-VCH, Weinheim*.
30. Ma X., and Song Q. (2020) Recent Progress on Selective Deconstructive Modes of Halodifluoromethyl and Trifluoromethyl-containing Reagents. *Chem. Soc. Rev.*, 49 9197-9219 (<https://doi.org/10.1039/D0CS00604A>).
31. Wang X., Lei J., Liu Y., Ye Y., Li J., and Sun K. (2021) Fluorination and Fluoroalkylation of Alkenes/Alkynes to Construct Fluorocontaining Heterocycles. *Org. Chem. Front.*, 8 2079-2109 (<https://doi.org/10.1039/D0QO01629B>).
32. Pokorny J. (2007) Are Natural Antioxidants Better – and Safer – Than Synthetic Antioxidants? *Eur. J. Lipid. Sci. Technol.*, 109 (6) 629-642 (<http://dx.doi.org/10.1002/ejlt.200700064>).
33. Stoia M., and Oancea S. (2022) Low-Molecular-Weight Synthetic Antioxidants: Classification, Pharmacological Profile, Effectiveness and Trends. *Antioxidants (Basel)*, 11 (4) 638 (<https://doi.org/10.3390/antiox11040638>).
34. Danyliuk I., Kovalenko N., Tolmachova V., Kovtun O., Saliyeva L., Slyvka N., Holota S., Kutrov G., Tsapko M., and Vovk M. (2023) Synthesis and Antioxidant Activity Evaluation of Some New 4-Thiomethyl Functionalized 1,3-thiazoles. *Curr. Chem. Lett.*, 12 (4) 667-676 (<https://doi.org/10.5267/j.ccl.2023.6.002>).
35. Pham-Huy L.A., He H., and Pham-Huy C. (2008) Free Radicals, Antioxidants in Disease and Health. *Int. J. Biomed. Sci.*, 4 (2) 89-96 (<https://doi.org/10.59566/IJBS.2008.4089>).
36. Bouayed J., and Bohn T. (2010) Exogenous Antioxidants—Double-Edged Swords in Cellular Redox State: Health Beneficial Effects at Physiologic Doses Versus Deleterious Effects at High Doses. *Oxid. Med. Cell. Longevity.*, 3 (4) 228-237 (<https://doi.org/10.4161/oxim.3.4.12858>).
37. Danyliuk I.Yu., Kemsykyi S.V., Polishchuk V.M., Shishkina S.V., and Vovk M.V. (2024) Visible-light-induced Photocatalytic Iododi(per)fluoroalkylation of 5-Amino-*N*-allyl-1,2,3-Triazole-4-Carboxamides. *J. Fluor. Chem.*, 276 110292 (<https://doi.org/10.1016/j.jfluchem.2024.110292>).
38. Marano S., Minelli C., Ripani L., Marcaccio M., Laudadio E., Mobbili G., Amici A., Armeni T., and Stipa P. (2021) Insights into the Antioxidant Mechanism of Newly Synthesized Benzoxazinic Nitrones: *In Vitro* and *In Silico* Studies with DPPH Model Radical. *Antioxidants.*, 10 (8) 1224 (<https://doi.org/10.3390/antiox10081224>).
39. Firsch M.J., Trucks G.W., and Schlegel H.B. (2016) Gaussian 09, Revision A.02, Wallingford CT.
40. Korkusuz E., Sert Y., Kılıçkaya Selvi E., Aydın H., Koca İ., and Yıldırım İ. (2023) Molecular Docking and Antioxidant Activity Studies of Imidodithiocarbonate Derivatives Containing Pyrimidine. *Org. Commun.*, 16 (1) 1-10 (<https://doi.org/10.25135/aeg.oc.143.2212.2658>).

41. Al-Balushi R.A., Al-Busaidi I.J., Al-Sharji H., Haque A., Faizi M.S.H., Dege N., Khan M.S., and Mohamed T.A. (2022). Synthesis, Structural, Photo-physical Properties and DFT Studies of Some Diarylheptanoids. *J. Mol. Struct.*, 1264 133254. (<https://doi.org/10.1016/j.molstruc.2022.133254>).
42. Gázquez J.L., Cedillo A., and Vela A. (2007) Electrodonating and Electroaccepting Powers. *J. Phys. Chem. A*, 111 (10) 1966-1970 (<https://doi.org/10.1021/jp065459f>).
43. Domingo L.R. (2024) 1999 – 2024, a Quarter Century of the Parr’s Electrophilicity ω Index. *Scientiae Radices*. 3 (3) 157-186 (<https://doi.org/10.58332/scirad2024v3i3a02>).
44. Pérez P., Domingo L. R., José Aurell M., and Contreras R. (2003) Quantitative Characterization of the Global Electrophilicity Pattern of Some Reagents Involved in 1,3-Dipolar Cycloaddition Reactions. *Tetrahedron*, 59 (17) 3117–3125 ([https://doi.org/10.1016/S0040-4020\(03\)00374-0](https://doi.org/10.1016/S0040-4020(03)00374-0)).
45. Domingo L.R., Chamorro E., and Pérez P. (2008) Understanding the Reactivity of Captodative Ethylenes in Polar Cycloaddition Reactions. A Theoretical Study. *J. Org. Chem.*, 73 (12) 4615–4624 (<https://doi.org/10.1021/jo800572a>).
46. El-Sheshtawy H.S., Ibrahim M.M., El-Mehasseb I., and El-Kemary M. (2015) Orthogonal Hydrogen/Halogen Bonding in 1-(2-Methoxyphenyl)-1*H*-imidazole-2(3*H*)-thione-I₂ Adduct: An Experimental and Theoretical Study. *Spectrochimica Acta Part A: Mol. Biomol. Spectroscopy.*, 143 (15) 120-127 (<https://doi.org/10.1016/j.saa.2015.02.043>).
47. Murray J.S., and Politzer P. (2011) The Electrostatic Potential: an Overview. *Wiley Interdiscip. Rev. Comput. Mol. Sci.*, 1 (2) 153-163 (<https://doi.org/10.1002/wcms.19>).
48. Trott O., and Olson A.J. (2010) AutoDock Vina: Improving the Speed and Accuracy of Docking with a new Scoring Function, Efficient Optimization and Multithreading. *J. Comput. Chem.*, 31 (2) 455-461 (<https://doi.org/10.1002/jcc.21334>).
49. Declercq J.-P., Evrard C., Clippe A., Stricht D.V., Bernard A., and Knoops B. (2001) Crystal Structure of Human Peroxiredoxin 5, a Novel Type of Mammalian Peroxiredoxin at 1.5 Å Resolution. *J. Mol. Biol.*, 311 (4) 751-759 (<https://doi.org/10.1006/jmbi.2001.4853>).
50. Brand-Williams W., Cuvelier M.E., and Berset C. (1995) Use of a Free Radical Method to Evaluate Antioxidant Activity. *LWT – Food Science and Technology.*, 28 (1) 25-30 ([https://doi.org/10.1016/S0023-6438\(95\)80008-5](https://doi.org/10.1016/S0023-6438(95)80008-5)).



© 2025 by the authors; licensee Growing Science, Canada. This is an open access article distributed under the terms and conditions of the Creative Commons Attribution (CC-BY) license (<http://creativecommons.org/licenses/by/4.0/>).